Mechanisms of Ageing and Development 207 (2022) 111722

Contents lists available at ScienceDirect

Mechanisms of Ageing and Development

journal homepage: www.elsevier.com/locate/mechagedev

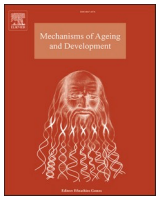

Mitochondrial DNA insertions into nuclear DNA affecting chromosome segregation: Insights for a novel mechanism of immunosenescence in mice

Mónica González-Sánchez [a,*], Víctor García-Martínez [a], Sara Bravo [a], Hikaru Kobayashi [a], Irene Martínez de Toda [a], Blanca González-Bermúdez [b,c], Gustavo R. Plaza [b,c], Mónica De la Fuente [a]

[a] Department of Genetics, Physiology and Microbiology, Facultad de Ciencias Biológicas, Universidad Complutense de Madrid, E-28040 Madrid, Spain
[b] Center for Biomedical Technology, Universidad Politécnica de Madrid, E-28223 Pozuelo de Alarcón, Spain
[c] Department of Materials Science, ETSI de Caminos, Canales y Puertos, Universidad Politécnica de Madrid, E-28040 Madrid, Spain

ARTICLE INFO

Keywords:
NUMTs
MtDNA
Micronuclei
Lymphoproliferation
Immunosenescence
Oxidative stress

ABSTRACT

Mitochondrial DNA sequences were found inserted in the nuclear genome of mouse peritoneal T lymphocytes that increased progressively with aging. These insertions were preferentially located at the pericentromeric heterochromatin. In the same individuals, binucleated T-cells with micronuclei showed a significantly increased frequency associated with age. Most of them were positive for centromere sequences, reflecting the loss of chromatids or whole chromosomes. The proliferative capacity of T lymphocytes decreased with age as well as the glutathione reductase activity, whereas the oxidized glutathione and malondialdehyde concentrations exhibited a significant increase.

These results may point to a common process that provides insights for a new approach to understanding immunosenescence. We propose a novel mechanism in which mitochondrial fragments, originated by the increased oxidative stress status during aging, accumulate inside the nuclear genome of T lymphocytes in a time-dependent way. The primary entrance of mitochondrial fragments at the pericentromeric regions may compromise chromosome segregation, causing genetic loss that leads to micronuclei formation, rendering aneuploid cells with reduced proliferation capacity, one of the hallmark of immunosenescence. Future experiments deciphering the mechanistic basis of this phenomenon are needed.

1. Introduction

It has been proposed that aging is caused by the cumulative damage produced by the constant generation of reactive oxygen species in the mitochondria (mitROS) throughout the life of the individuals (Harman, 1972). Although ROS production unrelated to cellular respiration occurs, such as in microsomes, peroxisomes or the membrane-bound NADPH-oxidase complex (Boveris et al., 1972; Vermot et al., 2021), the respiratory Mitochondrial Complex I, located on the cytosolic face of the mitochondria, is the main production focus of ROS (Sanchez-Roman and Barja, 2013). This fact is relevant because mitROS produced in this complex are directed to the matrix, closely affecting mitochondrial DNA (mtDNA) which is anchored to the internal mitochondrial membrane.

Histone-devoid mtDNA is more vulnerable than nuclear DNA to the damage produced by mitROS. Single and double-strand breaks occur (Brand, 2010) giving rise to fragments that show a higher level of oxidized DNA bases (Suter and Richter, 1999), a marker of ROS-induced DNA oxidative damage, supporting that the origin of the fragments is mainly mitROS attack, and not only deletions during the repair process or other causes.

Richter (1988) proposed that the mtDNA fragments generated by mitROS could escape from the mitochondria and insert into the nucleus, causing a time dependent nuclear accumulation responsible for aging. Patrushev et al. (2004), detected mtDNA fragments released from mitochondria through the permeability transition pore, a non-specific pore located at the inner membrane of this organelle described by Hunter and Haworth (1979). Whereas the migration of mtDNA sequences to the nucleus has played a key role in the evolution of eukaryotic organisms, different studies have shown that this is an ongoing process. This phenomenon, called numtogenesis (Singh et al.,

* Corresponding author.
E-mail address: mgs@ucm.es (M. González-Sánchez).

https://doi.org/10.1016/j.mad.2022.111722
Received 13 December 2021; Received in revised form 6 August 2022; Accepted 7 August 2022
Available online 9 August 2022

2017), in reference to the name given to mtDNA sequences in the nuclear genome (NUMTs: NUclear MiTochondrial DNA), has been observed in many different species (Puertas and González-Sánchez, 2020).

The genomic instability caused by mtDNA insertions into the nuclear genome has implications for the development of human pathologies such as Pallister Hall syndrome (Turner et al., 2003), different types of cancer and aging (Singh et al., 2017). Studies conducted in rats have shown that the amount of mtDNA in the nucleus increases with age in the liver and the brain (Caro et al., 2010). Similar results have been observed in yeasts, where the insertion of mtDNA fragments decreases chronological life span (Cheng and Ivessa, 2010, 2012). In addition, age-related numtogenesis in mice has been found to be related to mitROS production throughout the life of individuals, because the amount of mtDNA found in the hepatocyte nuclei of old mice decreased to levels similar to young individuals when treated for 7 weeks with rapamycin (Martínez-Cisuelo et al., 2016). This drug, which inhibits TOR (target of rapamycin) protein, decreases mitROS production at the Mitochondrial Complex I, and it has been described to be capable of increasing longevity in mammals (Harrison et al., 2009).

NUMTs are generally located at the centromeric and pericentromeric regions of chromosomes (Matsuo et al., 2005; Caro et al., 2010; Michalovova et al., 2013; Martínez-Cisuelo et al., 2016) where mtDNA fragments are introduced using the Non-Homologous End Joining (NHEJ) mechanism (Ricchetti et al., 1999; Hastings et al., 2009; Harutyunyan et al., 2020). (Peri)centromeric regions in mice are composed of the minor (MiSat) and major satellite (MaSat) sequences. They are made up of repeated sequences that occupy different, non-intermingled, chromosome domains (Garagna et al., 2002).

(Peri)centromeric regions are usually heterochromatic and transcriptionally inactive but play an essential role in the cohesion and dissociation processes that occur at centromeres during cell division (Guenatri et al., 2004). Although mtDNA sequences have been described at the (peri)centromeric regions, the effect that these insertions might have on chromosome segregation and cell division is yet to be clarified.

Fenech and Morley (1985) reported increased chromosome mis-segregation and micronuclei (MN) formation associated to age. They developed the Cytokinesis-Block MicroNucleus assay (CBMN assay) to perform in vitro analysis of DNA damage and chromosome loss in human lymphocytes from peripheral blood. CBMN assay is based on the use of cytocalasin-B (Cyt-B) that inhibits cytokinesis and renders easily recognizable binucleated (BN) cells in which micronuclei (MN) can be observed. MN are among the best markers to assess chromosomal instability (Fenech et al., 2003). They originate from both fragmented DNA and/or whole chromosome loss due to laggard chromosomes unable to reach the poles in the preceding mitosis, leading to aneuploid cells. Additionally, other cytological markers related to DNA damage, such as nucleoplasmic bridges (NPB) or cells with signs of apoptosis, can also be detected. CBMN assay has been further developed in combination with fluorescence in situ hybridization (FISH) using specific molecular probes to investigate centromere-positive MN (Migliore et al., 1996), providing a useful tool for the assessment of chromosome loss due to defective centromeres that fail to segregate properly.

The oxidation-inflammation theory of aging proposes that aging is the result of the establishment of a chronic oxidative and inflammatory stress situation in which immune cells play a fundamental role due to their persistent production of oxidant and inflammatory compounds (De La Fuente and Miquel, 2009). With age, the function of immune cells declines, a process that is known as immunosenescence (Pawelec, 2018) which is responsible for the age-related increase in morbidity and mortality (De La Fuente and Miquel, 2009). One of the most studied immune functions is the capacity of T lymphocytes to proliferate in response to an antigenic challenge, which is known to experience an age-related decrease (Martínez de Toda et al., 2016). Although it was proposed that the basis of this immune deterioration is oxidative stress (Moro-García et al., 2018; Martínez de Toda et al., 2021), the underlying mechanism responsible for this defective proliferative capacity is not known. Nevertheless, an age-related increase in an oxidative stress situation has been described in immune cells from humans and mice, with significant decreases of antioxidant defenses such as glutathione reductase activity and increases of oxidant compounds such as oxidized glutathione (GSSG) and products of lipid oxidative damage such as malondialdehyde (MDA) concentrations (Martinez de Toda et al., 2020).

Taking all this into account, the aim of this study is to provide insights for the causative effect of mitochondrial DNA insertions at the pericentromeric regions that, eventually affecting proper chromosome segregation, might be responsible for the reduced lymphoproliferation characteristic of immunosenescence. Moreover, whether these mitochondrial DNA insertions correlate with several oxidative stress parameters was also analyzed.

In this work we performed a longitudinal study based on the examination of mice T lymphocytes isolated from peritoneum without sacrifice, allowing monitoring each animal during the adult, mature and old age. Mitochondrial DNA insertions were quantified, and their chromosomal location was analyzed. Chromosome segregation failure and genetic loss was explored by means of the CBMN assay. In addition, we investigated the proliferative capacity of lymphocytes and several redox parameters such as glutathione reductase activity, oxidized glutathione (GSSG) and malondialdehyde (MDA).

2. Materials and methods

2.1. Animals and experimental conditions

Five ex-reproductive female mice (*Mus musculus*) of the outbred strain ICR-CD1, acquired from Janvier Labs (Germany) at the age of young adult (28 ± 4 weeks old) were used. The animals were housed under standard conditions of temperature (22 ± 1ºC) and humidity (50–60 %) with an inverted light: dark cycle (12 h: 12 h), light starting at 8:00 am. Mice had access to tap water and standard pelleted food (Envigo Teklad, Envigo, Madison WI, EEUU) ad libitum. To avoid alterations due to circadian cycles, the manipulation and sampling was carried out from 8:30 am to 12:00 pm.

The study carried out included a longitudinal analysis in which samples were taken from the peritoneum of the same animal at three different life stages: adult age (A, 40 ± 4 weeks), mature age (M, 56 ± 4 weeks) and old age (O, 71 ± 4 weeks). Analysis was made individually, monitoring each parameter during the aging process of each individual.

The protocols performed were approved by the Animal Experimentation Committee of the Complutense University of Madrid. The animals were treated according to the guidelines indicated by the European Community Council 2010/63 / EU.

2.2. Peritoneal leukocyte extraction and T-lymphocyte enrichment

Samples of peritoneal leukocytes were extracted following the method previously described by Martinez de Toda et al. (2016). Briefly, mice were immobilized by the scruff of the neck and 2 ml of sterile, 37ºC prewarmed, Hank's buffer were intraperitoneally injected. After gentle abdominal massage, approximately 80 % of the medium was recovered.

Peritoneal extractions were deposited on MIF plates (Macrophage Inhibitor Factor, Kartell) previously sterilized by 45 mins of UV exposure, and incubated 45 mins in sterile conditions at 37ºC, 5 % of CO_2 and humidified atmosphere. T-lymphocytes enriched supernatants were collected and quantified for viable cell density by Trypan Blue exclusion test using a Neubauer cell counting chamber and an optical microscope. Supernatants were adjusted to 10^6 lymphocytes/ml with RPMI 1460 (HyClone) supplemented with 1 mg/ml gentamicin (Sigma-Aldrich) and 10 % decomplemented Fetal Bovine Serum (FBS, MPBio).

2.3. Mitochondrial fragment quantification in T-lymphocyte nuclei

T-lymphocyte enriched suspensions were fixed in a solution of methanol: acetic acid (3: 1 v / v) and 20 ml were dropped onto clean glass slides and air-dried overnight.

2.3.1. Probes

Total DNA was isolated from peritoneal T lymphocytes using the FlexiGene® kit (Qiagen) and both MaSat and MiSat sequences and a 1841 bp mitochondrial fragment were amplified by PCR to generate the probes for in situ hybridization.

The synthetic oligonucleotides F-GGA CCT GGA ATA TGG CGA GAAA and R- TTC AGT GTG CAT TTC TCA TTTT (CONDA) were used to amplify the MaSat sequence in a touch-down PCR program consisting of 20 cycles of 30 s at 95ºC and 90 s at 67ºC (temperature decreasing 0.5ºC each cycle) and 15 cycles of 30 s at 95ºC and 90 s at 63ºC, and a final step of 7 min at 72 °C. For MiSat DNA amplification, the F-CAATGAGTTA-CAATGAGAAACATGG and R-TGATATACACTGTTCTACAAATCCCG oligonucleotides (CONDA) were used. The touch-down PCR program included 30 cycles of 30 s at 95ºC, 60 s at 57ºC (temperature decreasing 0.5ºC each cycle) and 60 s at 72ºC and 15 cycles of 30 s at 95ºC and 60 s at 55ºC.

Mitochondria from hepatocytes belonging to mice of the same strain as the individuals under study were isolated according to the method of Rickwood et al. (1987) and total mtDNA was extracted following the method described in Latorre et al. (1986). The F-CCACTCATTCATT-GACCTACCTGCC and R-TAGGTGATTGGGTTTTGCGGACTA primers (CONDA) were used to amplify a 1841 bp-long mitochondrial sequence fragment following the method described in Patrushev et al. (2004), who reported the presence of this fragment in the cytoplasm of irradiated mice. The PCR program used was: 3 mins at a temperature of 95 °C followed by 20 cycles of 95 °C for 30 s, 65ºC for 1 min and 30 s, 15 cycles of 95 °C for 30 s and 60 °C for 1 min and 30 s, and a final step of 72ºC for 7 mins.

Vertebrate telomere sequence (TTAGGG)n was amplified by PCR following the method described in Ijdo et al. (1991) using the primers: 5'-$(TTAGGG)_5$-3' and 5'-$(CCCTAA)_5$-3' (CONDA) in the absence of genomic DNA template. The PCR program was an initial 5 mins denaturation step at 95 °C followed by 10 cycles of 95ºC for 1 min, 55 °C for 30 s and 1 min and 30 s at 72ºC, continued by 30 cycles of 95ºC for 1 min, 30 s at 60 °C and 1.5 mins at 72ºC.

Amplification products were purified using the QIAquick® PCR Purification Kit (Qiagen) and labelled by nick translation with Tetramethyl-Rhodamine-5-dUTP (red) (Sigma Aldrich) and Fluorescein-12-dUTP (green) (Sigma Aldrich) using the Nick Translation Mix kit (Roche).

2.3.2. Sequencing of amplification products

The purified amplification products were sequenced by the Genomic Unit of the Genomics and Proteomics Research Support Center of the Complutense University of Madrid (UCM) and searched in BLAST © (Basic Local Alignment Search Tool) database (https://blast.ncbi.nlm.nih.gov/Blast.cgi) for homology.

2.3.3. Fluorescence in situ hybridization (FISH)

Slides were incubated with RNAsa 1 μg/ml, Sigma) in 2XSSC for 1 h at 37ºC, rinsed twice in 2XSSC for 5 min and incubated in 0.12 % pepsin for 15 mins at 37ºC. They were washed twice in PBS for 5 min each, rinsed in 2XSSC 5 min, fixed in 4 % paraformaldehyde (SIGMA) for 10 min and washed tree times in 2XSSC for 5 mins each. Slides were sequentially dehydrated in a series of 70 %, 90 % and 100 % ethanol, air dried for 30–75 min and denatured in 70 % (v/v) formamide for 15 min at 80ºC. The hybridization mixture containing 2 ng of each labelled probe in 50 % (v/v) formamide, 20 % (v/v) dextran sulfate in 2XSSC, was denatured 10 min at 95ºC and quenched on ice 7 min. Slides were incubated with the hybridization mixture in a moist chamber for 24 h at 37ºC. Posthybridization washes were done in 50 % formamide in 2XSSC twice, followed by two washes in 2XSSC, 5 min each at 45ºC.

Cells were simultaneously counterstained with 4', 6-diamidine-2-phenylindole (DAPI) and mounted in Vectashield (H- 1200, Vector Laboratories) and stored at 4ºC until observation.

Slides from the same mice at each of the three different ages (A, M and O) were observed with an Olympus BX60 epiflourescence microscope equipped with a motorized Z axis. Images were captured with an Olympus CCD DP70 digital camera attached to the microscope, at a resolution of 4080 × 3072 pixels, using the DP Manager and DP Controller software package (Soft Imaging System, Olympus). Red and green images were acquired every 0.5 μm in the Z axis, at a constant exposure time, in the same contrast and brightness camera conditions. Image stacks of 50 nuclei per individual and age were obtained.

2.3.4. Quantitative FISH

Measurements of fluorescence signals were performed with the open-source ImageJ software (http://rsb.info.nih.gov/ij). Color stacks were converted into 2D 8-bit grayscale images and the region of interest was selected following the contour of the DAPI-stained nucleus. Both the area and intensity of each signal were calculated as the product of the number of pixels belonging to each signal and a number between 0 and 255, corresponding to the 256 levels of the grey scale in an 8-bit image, 0 being the absence of fluorescence, in each cell. Data were collected and exported to Microsoft® Excel® for further analysis.

2.4. CBMN assay

T-lymphocyte enriched suspensions were seeded 200 μl/well into 96-well plates (Costar, Cambridge, MA, USA) and placed in a sterile incubator at 37ºC with 5 % CO_2 and humidified atmosphere. Mitosis was induced by addition of 20 μl Concanavalin A (Con A), a lectin for stimulating T-cell proliferation. (Sigma-Aldrich) at a final concentration of 1 μl/ml. Binucleated cells were obtained using the method previously described by Fenech (Fenech, 2007) with a few changes. After 18 h of incubation, cytokinesis was inhibited by adding cytochalasin-B (Cyt-B) at a final concentration of 4.5 μl/ml. After 26 h, cells were collected, fixed in methanol: acetic acid (3: 1 v / v) and stored at 4ºC until use.

Cell suspensions were dropped onto glass slides, allowed to air dry and stained with hematoxylin and eosin staining. Slides were observed with an optical microscope at 40X magnification. About 1500 cells per individual in each of the three ages were analyzed and the following parameters were calculated according to criteria described in Fenech et al. (2003):

- Micronucleated (MNed) binucleated (BN) cell frequency:
  MNed BN freq= (*number of BN cells with at least one micronucleus)/* T_{BN}
- Mean number of micronuclei (MN) in MNed BN cells:
  MN mean number = (*MN1 +2 *MN2 +3 *MN3 +4 *MN4)/* $T_{MNed\ BN}$
- Nucleoplasmic bridges (NPB) frequency:
  NPB= *number of cells with at least one NPB /* T_{BN}
- Frequency of apoptotic cells (APO):

APO= *number of cells showing late-stage apoptotic cytological signs/ N.*

Where MN1-MN4 represents the number of BN cells with 1–4 micronuclei, respectively, T_{BN} *is the total of BN cells (with and without MN),* $T_{MNed\ BN}$ *is the total MNed BN cells and N is the total number of cells analyzed.*

2.5. FISH in MNed BN cells

To further study the composition of MN, 300 MNed BN cells were analyzed by FISH using a commercial fluorescein-labelled pancentromeric mouse sequence (StarFISH) as probe, in combination with vertebrate telomere sequence (TTAGGG)n labelled with rhodamine. The FISH

protocol described above was followed. Slides were stored at 4ºC in darkness for subsequent observation using an Olympus BX60 epifluorescence microscope equipped with the appropriate filters for the detection of the different fluorochromes used. Images were taken at 100X magnification with the Olympus CCD DP70 camera attached to the microscope, using the DP Manager and DP Controller software package. Photographs were processed using the Adobe Photoshop CS5 Extended image editing software.

MNed BN cells were observed and the frequency of centromere-positive MN (Cen + MN) was scored as:

Cen+ MN= MNC1 + 2 *MNC2 + 3 *MNC3 + 4 *MNC4/ 1 *MN1 + 2 *MN2 + 3 *MN3 + 4 *MN4.

Where MNC1-MNC4 represents the number of BN cells with 1–4 centromere-positive MN and MN1-MN4 the number of BN cells with 1–4 micronuclei.

2.6. Lymphoproliferation

The proliferation capacity of T lymphocytes was evaluated by the method previously described (Martinez de Toda et al., 2016). Peritoneal cell suspensions were adjusted to 5×10^5 lymphocytes/ml in complete medium containing RPMI-1640, 10 % fetal bovine serum and 1 % gentamicin. 200 µl containing 1 × 105 lymphocytes were dispensed into 96-well plates. 20 µl/well of Con A (1 µg/ml) was added for stimulating proliferation. The plates were incubated at 37ºC in a sterile and humidified atmosphere of 5 % CO_2 for 48 h. Then, 100 µl of culture supernatants were removed and 100 µl of fresh medium was added to each well together with 2.5 µCi ^{3}H-thymidine (Hartmann Analytic, Germany), followed by another incubation of 24 h. Cells were harvested in a semiautomatic harvester (Skatron Instruments, Norway) and thymidine uptake was measured in a beta counter (LKB, Upsala, Sweden) for 1 min. The results are expressed as counts per min (cpm) reflecting ^{3}H-thymidine uptake, which directly measures proliferation of lymphocytes after Con A stimulation.

2.7. Redox parameters examination

2.7.1. Glutathione reductase (GR) Activity

The activity of the antioxidant enzyme glutathione reductase (GR) was evaluated in peritoneal leukocytes following a method previously described (Martínez de Toda et al., 2019, 2020). Leukocytes were adjusted to 10^6 total cells/ml in Hank's medium and centrifuged, and the cell pellets were resuspended in oxygen-free phosphate buffer 50 mM and EDTA 6.3 mM. Then, they were sonicated, and supernatants were used for the enzymatic reaction together with oxidized glutathione (GSSG) 80 mM as substrate, as previously described. Oxidation of NADPH was measured at 340 nm. The results were expressed as units (U) of GR activity/mg protein.

2.7.2. Oxidized Glutathione (GSSG) Concentration

Peritoneal leukocyte concentrations of oxidized glutathione (GSSG) were analyzed following a method previously described (Martínez de Toda et al., 2019, 2020). Cells were adjusted to 10^6 total cells/ml in Hank's medium and centrifuged, and cell pellets were resuspended in phosphate buffer 50 mM and EDTA 0.1 M, pH 8. Then, they were sonicated, and supernatants were used for the quantification of oxidized glutathione (GSSG) by the reaction capacity that GSSG have with o-phthalaldehyde (OPT) at pH 12, resulting in the formation of a fluorescent compound. Fluorescence was measured at 350 nm excitation and 420 nm emission. Results were expressed as nmol of GSSG/mg protein.

2.7.3. Malondialdehyde (MDA) Concentration

Concentrations of MDA were evaluated using the commercial kit "Lipid Peroxidation (MDA) Assay Kit" (BioVision, CA, USA). Peritoneal leukocytes were adjusted to 10^6 total cells/ml in Hank's medium and centrifuged and cell pellets were resuspended in MDA lysis buffer. Then, they were sonicated, and supernatants were incubated with thiobarbituric acid (TBA) for 60 min in a water bath. Then, samples were centrifuged, and supernatants collected and dispensed into 96-well plates for spectrophotometric measurement at 532 nm, as previously described (Martínez de Toda et al., 2019, 2020). Results were expressed as nmol MDA/mg protein.

2.8. Statistics

All statistical analyses and tests were performed with the IBM® SPSS® Statistics 21 program (SPSS, Chicago, IL, USA). Differences in mtDNA signals were analyzed using the non-parametric Kruskall-Wallis test followed by the Mann-Whitney-Wilcoxon test for paired comparisons. For the remaining data, one-way ANOVA followed by a post hoc analysis of Scheffe was applied. Differences between age groups were studied through Student́s t-test for paired samples. The Pearson correlation coefficient was used to test for correlation between variables. Two-sided $P < 0.05$ was considered the minimum level of significance.

3. Results

A longitudinal study was carried out in which peritoneal leukocytes from the same individual were analyzed at three different moments of life: adult (40 ± 4 weeks), mature (56 ± 4 weeks) and old (71 ± 4 weeks) ages. Therefore, the experimental design allows to study each animal individually, monitoring each parameter during its aging process.

3.1. Analysis of the amplified sequences

Sequences amplified by PCR and later used as probes in the FISH procedure were analyzed using the BLAST© NCBI tool. Results revealed that the sequence amplified with MaSat-specific primers had 94 % homology with the 240 bp sequence "Mouse satellite DNA sequence" ID: V00846 annotated in the GenBank. On the other hand, the amplified sequence with MiSat-specific primers showed 100 % homology with the 121 bp sequence "Mouse centromeric minor satellite DNA (8)" ID: X14466.1. Analysis of the amplified mtDNA sequence revealed 100 % homology with a region of 1841 bp of the entire mitochondrial mouse genome (ID: KY018919.1). This sequence, referred to as 1841MT hereafter, is between the positions 14,189–16,029 of the mouse mitochondrial genome and comprises a region of the D-loop as well as part of the gene for cytochrome b, a component of complex III of the respiratory chain. The alignment of 1841MT with MiSat and MaSat sequences determined there was no similarity between the mtDNA sequence and mouse centromere satellite sequences.

3.2. Mitochondrial DNA sequences are present at the pericentromeric region of T-lymphocytes chromosomes and increase with age

The presence of the 1841MT sequence in the T-lymphocyte nuclei was confirmed by FISH and visualized as numerous mtDNA labels mainly located at definite loci (Fig. 1A_1, 1$B_{1–2}$, 1$D_{1–2}$) co-localizing to chromocentres (positive DAPI regions originated by the cytological association of the centromeres of several chromosomes).

To further analyze the chromosomal location of this mitochondrial fragment, 1841MT in combination with MaSat and MiSat probes were hybridized to metaphase chromosomes of colchicine-treated T lymphocytes. The results revealed the presence of the mtDNA fragment at the (peri)centromeric regions of each of the 40 telocentric female mouse chromosomes (Fig. 1$A_{1–4}$), where major and minor satDNA occupy two different chromosome domains (Fig. 1$B_{1–2}$, 1$D_{1–4}$), as already described (Garagna et al., 2002). Double FISH using both MaSat or MiSat probes simultaneously with 1841MT in interphase T- lymphocytes, where chromatin is less condensed, showed that the mitochondrial DNA

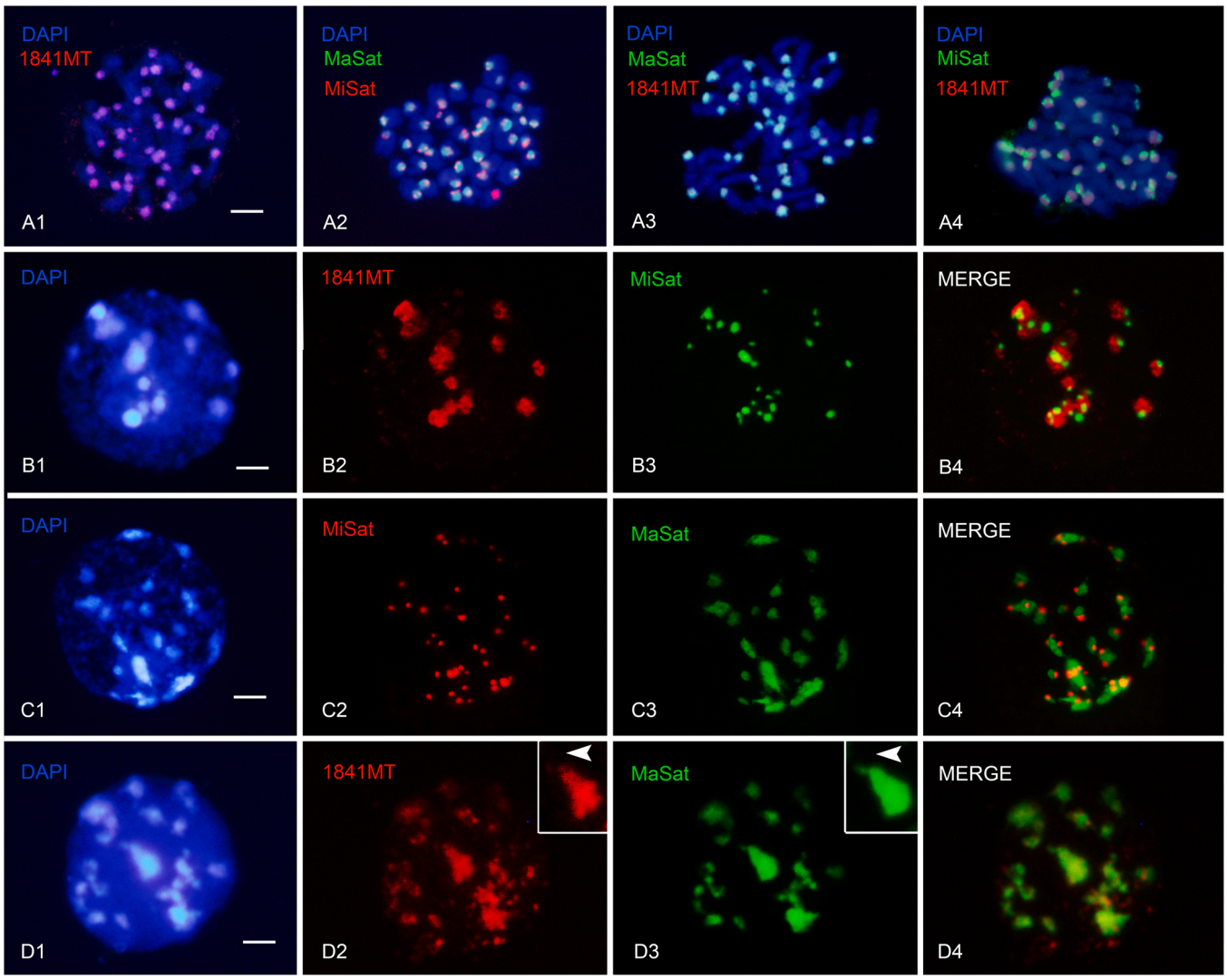

Fig. 1. Fluorescence in situ hybridization (FISH) micrograph of mice T lymphocytes using the mitochondrial DNA sequence (1841MT) and minor and major satellite-DNA (MaSat and MiSat) probes (red and green) showing their relative locations. Chromosomes were stained by 4', 6- diamidino-2- phenylindole (DAPI, blue). A: metaphase chromosomes from colchicine-treated cells. B-D: interphase nuclei. Bar = 2 μm.

sequence and minor satDNA are present in different centromere regions (Fig. 1B_{1-4}), whereas 1841MT and MaSat probes co-localize (Fig. 1D_{1-4}), although the major satellite DNA spans a broader area (fig D_2, D_3, arrowhead in insets).

To quantify the 1841MT signals observed in interphase lymphocyte nuclei from mice peritoneal liquid at the three different ages (A, M and O), total fluorescence per nucleus was measured in a quantitative FISH experiment. Considering that the degree of chromatin compaction (and therefore the intensity of the signals) may vary in each cell, individual or age group, MiSat probe was simultaneously used as a control in the same experiment. The relative fluorescence of 1841MT signals per nucleus (Rf 1841MT) was calculated as the ratio "1841MT total fluorescence/ MiSat total fluorescence" (Table 1). Results indicated a progressive increase in Rf 1841MT associated to age ($p < 0.000$). A paired comparison showed significant differences between A and O ages ($p < 0.000$), whereas at the mature age animals exhibited intermediate mean values between the values observed in the same mice at A and O ages.

3.3. Micronucleated binucleated cell frequency increases with age

CBMN assay allowed detection of mice micronuclei and nucleoplasmic bridges in binucleated cells, indicators of chromosome

Table 1
Mean values and standard errors at the adult (40 ± 4 weeks old), mature (56 ± 4 weeks old) and old (71 ± 4 weeks old) ages: the relative fluorescence of 1841MT signals per nucleus (Rf 1841MT), the micronucleated binucleated cell (MNed BN) frequency, the micronuclei (MN) number in micronucleated binucleated cells (MNed BN), the nucleoplasmic bridge (NPB) frequency and the frequency of cells with cytological signs of late-stage apoptosis (Apo frequency). 250 cells per age were analyzed for Rf1841MT quantification and 1500 cells per individual for the rest of the parameters; a: significantly different from the adult group, b: significantly different from the mature group, * $p < 0.01$, * * $p < 0.001$, * ** $p < 0.0001$.

Age group	Rf 1841MT	MNed BN frequency	MN number in Mned BN	NPB frequency	Apo frequency
ADULT	5.625 ± 0.101	0.393 ± 0.022	1.474 ± 0.069	0.033 ± 0.005	0.007 ± 0.002
MATURE	6.061 ± 0.133	0.442 ± 0.029	1.428 ± 0.012	0.049 ± 0.020	0.008 ± 0.002
OLD	6.674 ± 0.183^{a***}	0.505 ± 0.024^{a**}	1.486 ± 0.075	0.063 ± 0.005	0.012 ± 0.003$^{a*, b*}$

instability and DNA damage, as well as T lymphocytes exhibiting late apoptotic cytological signs (Fig. 2).

BN cells were scored for MN quantification. Both the frequency of MNed BN cells and the mean number of MN in MNed BN cells in each of the ages are summarized in Table 1. MNed BN cells showed a statistically significant increased frequency associated to age ($p = 0.027$), differences were found between adult and old ages ($p = 0.008$), whereas at mature age mice showed an intermediate value. Non-significant differences related to age were found for the mean number of MN in MNed BN cells.

BN cells were also scored for NPB formation. Although a tendency for NPB frequency to increase was noticed (Table 1), differences between ages were nonsignificant. Interestingly, the mean frequency of NPBs (0.048) was one order of magnitude lower that the mean frequency of MNed BNed cells (0.447).

T lymphocytes with apoptotic chromatin bodies within an intact cytoplasm characteristic of late-stage apoptosis were also scored and their frequency compared in the three moments of life. A small but statistically significant increase was observed associated to age ($p = 0.045$), the highest values being shown at the old age (Table 1).

3.4. MN composition reveals an aneugenic origin

To elucidate if MN are caused by DNA fragmentation or chromatid/chromosome loss (clastogenic or aneugenic origin, respectively), FISH using a mouse pancentromeric probe was performed in 300 MNed BN lymphocytes (Fig. 3). The frequency of centromere-positive MN found was 0.957 suggesting that, in most cases, MN may comprise complete lost chromatids or whole chromosomes. MN showing two telomere signals were also found (Figs. C1–2), supporting the idea that the origin of MN in the studied peritoneal lymphocytes could be mainly due to chromosome loss rather than DNA fragmentation.

3.5. Lymphocyte proliferation capacity decreases with age

The proliferation capacity of lymphocytes in response to Con A was assessed at the A, M and O ages. The results obtained are summarized in Table 2. A one-way ANOVA comparing the data belonging to the three different ages revealed a significant proliferation capacity reduction related to age ($p = 0.000$). A paired comparison showed significant differences between A and M ($p = 0.000$), A and O ($p = 0.000$) and M and O ($p = 0.001$).

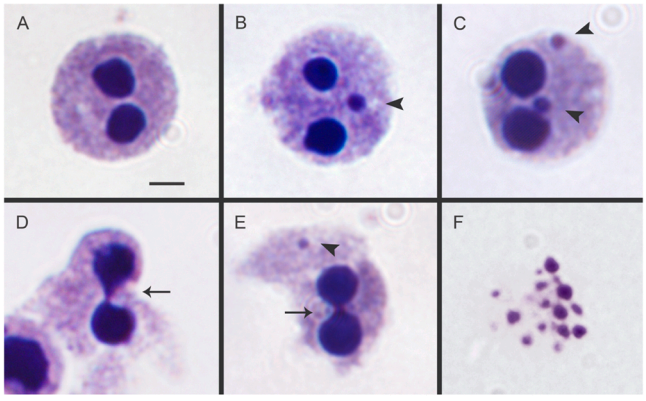

Fig. 2. Binucleated (BN) cells with hematoxylin and eosin staining. (A, B and C) BN cells with 0, 1 and 2 micronuclei (MN), respectively; (D) BN cell exhibiting a nucleoplasmic bridge (NPB); (E) BN cell with 1 MN and 1 NPB; (F) T lymphocyte with cytological signs of late-stage apoptosis. MN are indicated by arrowheads and NPBs by arrows. Bar= 3 μm.

3.6. Old animals showed less GR activity and more concentration of the oxidants GSSG and MDA

The results of the redox parameters: GR activity, GSSG and MLA concentrations, quantified in the three groups, are shown in Table 2. The activity of the antioxidant enzyme GR decreased with age ($p = 0.0013$). Significant differences were found between A and M (0.012), A and O (0.0013) and M and O (0.018) ages.

On the contrary, both GSSG and MDA concentrations showed a significant increase with aging ($p = 0.0000$ and 0.0007, respectively). Significant differences were found in a pair-comparison test between A and M, A and O and M and O ages.

3.7. Numtogenesis positively correlates with micronuclei frequency whereas both parameters are negatively related to lymphocyte proliferation capacity

For interrelation study, Pearson's correlation coefficients were calculated among the investigated parameters: Rf 1841MT, MNed BN cell frequency, mean number of MN in MNed BN cells, NPBs frequency, apoptosis and proliferation capacity of lymphocytes. A positive correlation between Rf 1841MT and MNed BN cell frequency ($R = 0.697$; $p < 0.01$) was found. Moreover, both parameters negatively correlate with the proliferation ability of lymphocytes ($R = -0.538$; $p < 0.05$ for Rf 1841MT and $R = -0.721$; $p < 0.01$ for MNed BN cell frequency; Fig. 4). Non-significant correlations were found among the rest of the parameters analyzed.

3.8. Numtogenesis negatively correlates with antioxidant enzymatic activity and positively with oxidant parameters

Pearson's correlation coefficients were also calculated between Rf 1841MT and each of the redox parameters: GR activity, GSSG and MDA concentration. Results showed a negative correlation between Rf 1841MT and GR activity ($R = -0.673$; $p < 0.01$) whereas a positive relation was found between Rf 1841MT and both GSSG and MDA concentrations ($R = 0.604$; $p < 0.05$ and $R = 0.661$; $p < 0.01$, respectively; Fig. 5).

4. Discussion

Our results show for the first time the presence of mitochondrial sequences in the nuclear genome of mouse T lymphocytes that increase with age. The longitudinal study carried out from the peritoneum allows the observation of this phenomenon during the aging process of each animal, providing individual results that might otherwise be overlooked in a population study. Female mice were used because this sex is more adequate to cohabitation studies since females are less aggressive and dominant than males; these behaviors could interfere with the results obtained from the parameters studied (Garrido et al., 2018).

We detect a 1841 bp mitochondrial sequence (1841MT) located at definite *loci* in the nuclei of lymphocytes from adult to old ages. The amount of 1841MT increases gradually, resulting in significant differences between the adult and the old ages. Previous works have shown numtogenesis associated to age in yeast (Cheng and Ivessa, 2010, 2012) and mouse liver and brain cells (Caro et al., 2010; Martínez-Cisuelo et al., 2016). Gene disruption caused both by *de novo* insertions or rearrangements of integrated mtDNA, such as duplications or transposon mediated fragmentation, (Shay and Werbin, 1992; Turner et al., 2003; Ricchetti et al., 2004; Hazkani-Covo et al., 2010) is the basis of the genome instability that contributes to senescence. Although we cannot conclude whether it is due to the transfer of newly originated fragments, amplification of integrated mitochondrial sequences or both, the increase in mtDNA amount that we observe during aging in the analyzed animals may be considered one of the mechanisms underlying immunosenescence.

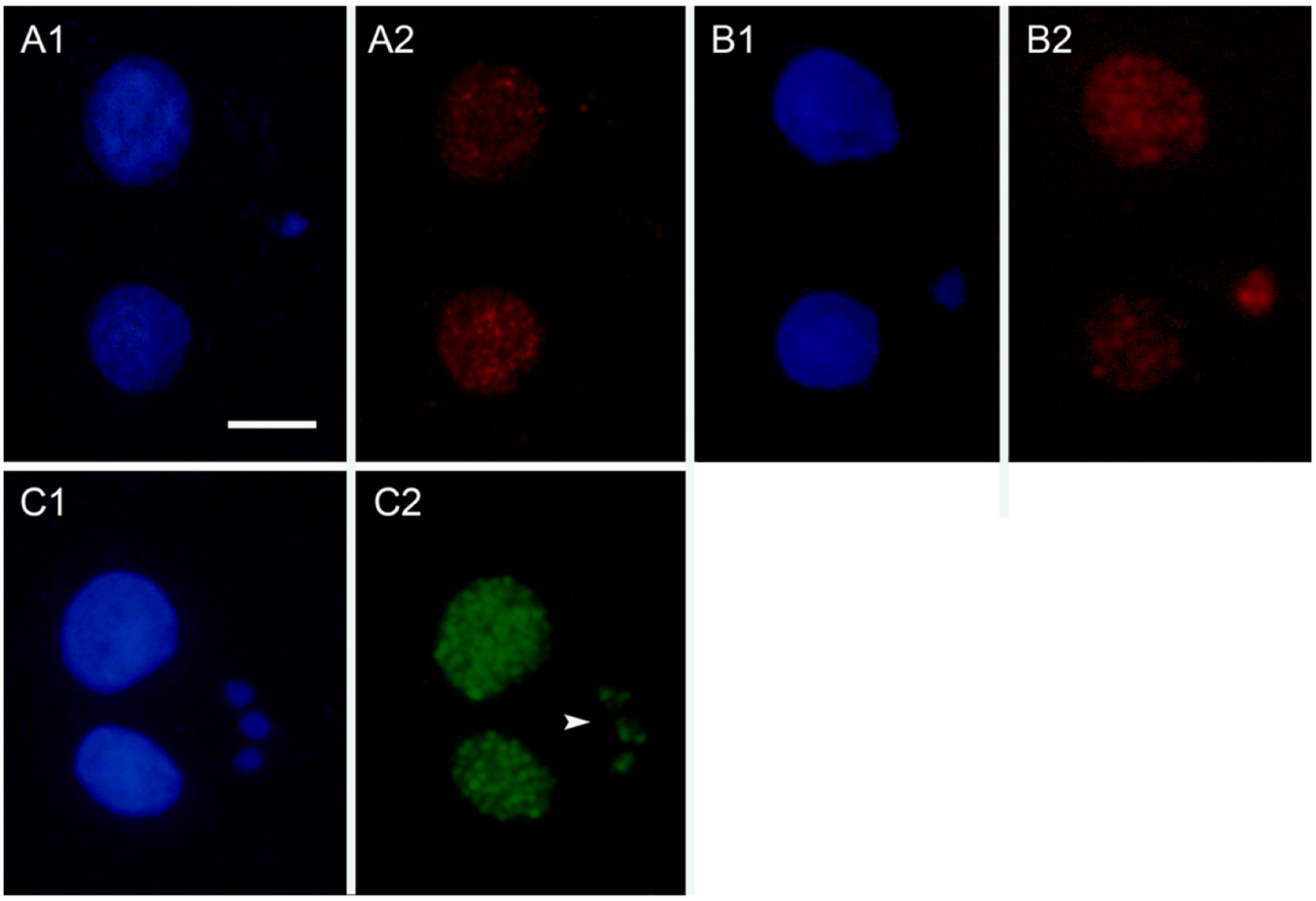

Fig. 3. FISH in binucleated (BN) cells showing micronuclei (MN) using a mouse pancentromeric probe (A2 and B2, red) and the specific probe for vertebrate telomeres (C2, green). (A1, B1 and C1) BN cells stained with 4', 6-diamidine-2-phenylindole (DAPI). (A1–2) BN cell with a centromere-negative MN; (B1–2) BN cell with a centromere-positive MN; (C1–2) BN cell with tree MN, each or them showing two telomere signals (arrowhead). Bar= 3 μm.

Table 2
Mean values and standard errors at the adult (40 ± 4 weeks old), mature (56 ± 4 weeks old) and old (71 ± 4 weeks old) ages: lymphoproliferation, the Glutathione Reductase (GR) activity, the Oxidized Glutathione (GSSG) and the Malondialdehyde (MDA) concentrations. Cpm: counts per min. 500,000 cells per individual were analyzed; a: significantly different from the adult group, b: significantly different from the mature group, * $p < 0.01$, * * $p < 0.001$, * ** $p < 0.0001$.

Age group	Lymphoproliferation (cpm)	GR activity (U GR/mg protein)	GSSG concentration (nmol GSSG/mg protein)	MDA concentration (nmol MDA/mg protein)
ADULT	4618 ± 126	26.710 ± 5.143	0.150 ± 0.04	1.788 ± 0.452
MATURE	3522 ± 62^{a***}	20.406 ± 3.925^{a*}	0.248 ± 0.04^{a**}	2.470 ± 0.237^{a*}
OLD	2657 ± 263$^{a***, b**}$	13.800 ± 3.074$^{a**, b*}$	0.318 ± 0.03$^{a***, b*}$	3.612 ± 0.801$^{a**, b*}$

FISH in colchicine-treated cells reveals chromosomal localization of 1841MT fragment at the centromeres of all autosomes and X chromosome in female mice. The fact that large blocks of 1841MT are already visible in the adult age suggests that this mitochondrial sequence may be constitutive, being present in several copy numbers as a part of the sequences found at the vicinity of centromeres. Organelle DNA, both mitochondrial and plastid, is often found at pericentromeric regions of many species (Puertas and González-Sánchez, 2020). This chromosome location provides a stable genomic environment for integration because it is a gene-poor region with frequent DSBs that are repaired by the NHEJ mechanism that allows fragments entrance (Matsuo et al., 2005). Once in the nuclear genome, organellar DNA can be fragmented by the insertion of transposon elements and reshuffled to different chromosome locations, resulting in a dynamism that contributes to genome instability (Michalovova et al., 2013).

Even though centromeres are the key for mtDNA to enter the nucleus, the effects of mitochondrial fragment integration in centromere function have not been elucidated. Although centromere identity is epigenetically defined and there is not a canonical conserved sequence among species, most centromeres are made up of arrays of repetitive satellite DNA (Fukagawa and Earnshaw, 2014). In mouse centromeres, MiSat sequences are present as a small block located at the centromeric region followed by a pericentromeric long cluster of MaSat, both being interrupted by short stretches of two GC-rich sequences (M3 and M4), resulting in two different domains with different functions during the process of chromosomal segregation. In addition to these four sequences, some other sequences exist that had not been described to date (Kuznetsova et al., 2006)

Our results show that 1841MT sequence is also part of the mouse centromeres. Double FISH using 1841MT in combination with MiSat and MaSat probes allows us to determine that this mitochondrial DNA fragment is located at the pericentromeric region, occupying a large area of the MaSat domain. From our cytological observations, 1841MT and MaSat seem to be intermingled, however high-resolution FISH on

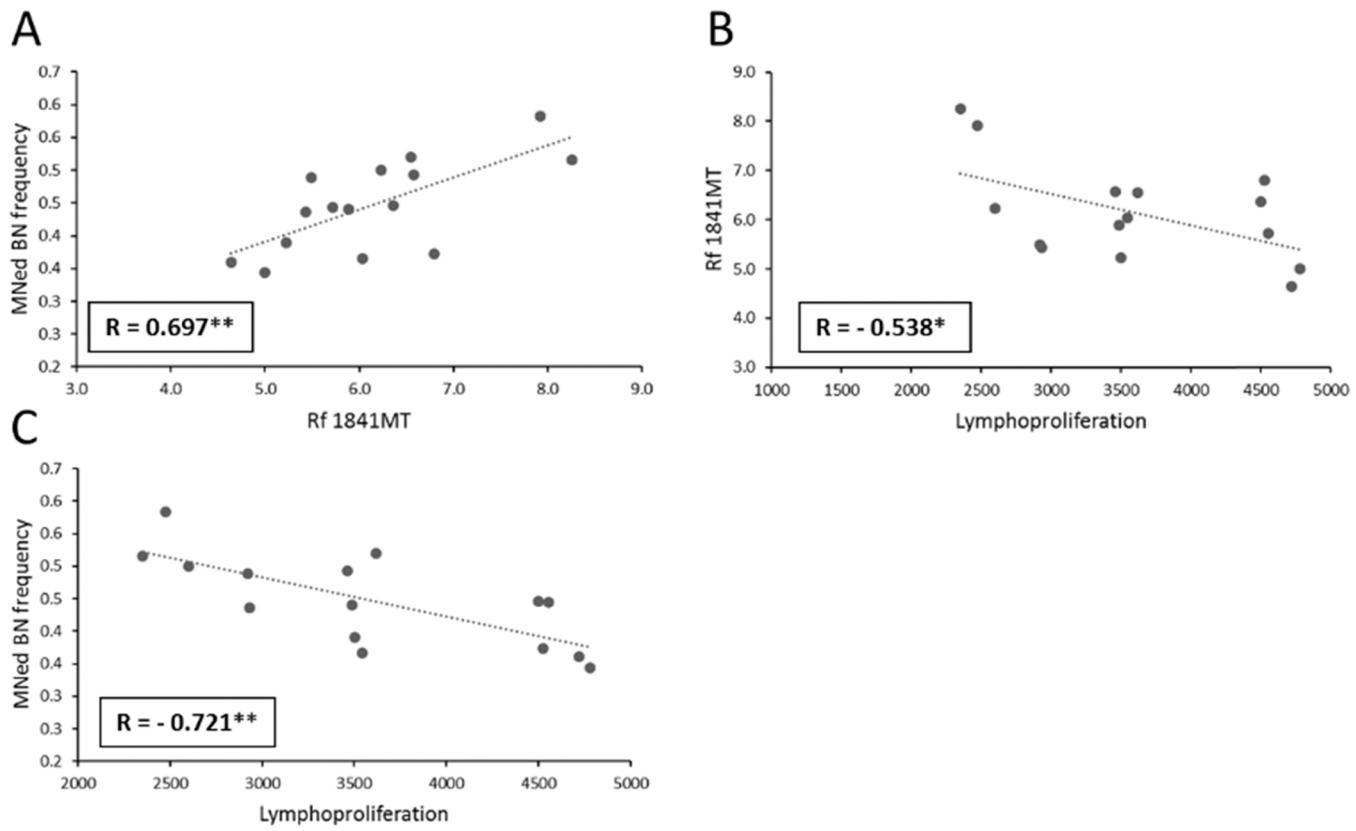

Fig. 4. Relationship between A) mtDNA relative fluorescence (Rf 1841MT) and micronucleated binucleated cell frequency (MNed BN frequency), B) Rf 1841MT and lymphoproliferation, C) MNed BN frequency and lymphoproliferation. R=Pearsońs correlation coefficient; * : $p < 0.05$; **: $p < 0.01$.

released chromatin (Fiber-FISH) will allow to deepen the future study of mouse (peri)centromeric DNA organization.

(Peri)centromeric heterochromatin plays a crucial role in chromosome segregation during cell division. Whereas MiSat domain constitutes the place for kinetochore nucleation and microtubule interaction, MaSat sequences are involved in maintaining sister-chromatid cohesion close to the centromere. The distinct roles of MiSat and MaSat domains cooperate in the cohesion and dissociation processes that occur during cell division to ensure proper chromatid segregation (Peters et al., 2001, 1982). It is likely that the genome instability generated by insertion and/or amplification of mitochondrial DNA sequences at the pericentromeric region causes age-associated disturbances that will affect centromeric function and/or sister-chromatid cohesion. Although 1841MT involvement in this phenomenon has not been investigated in this current study, a deeper understanding of its implication should be the subject of future research. Furthermore, smaller fragment integration undetected with FISH resolution in other regions different from centromeres, and affecting lymphocyte function, is also possible.

An improper centromeric function compromises correct segregation and predisposes the chromosome to premature chromatid separation, chromosome lagging and chromatid non-disjunction in aged cells (Pellestor et al., 2003; Liu and Keefe, 2008). Both laggard chromosomes and chromosomal fragments that fail to reach daughter nuclei during cell division appear as MN in the cytoplasm, resulting in uneven genetic material distribution and increased aneuploidy (Catalán et al., 1995, 2000; Cottliar and Slavutsky, 2001). Whereas genomic instability is a hallmark of aging as already mentioned, MN formation is considered one of the best validated biomarkers of chromosome instability related to aging (Fenech et al., 2020). Other nuclear abnormalities are also found with MN such as NPBs, a phenomenon that reveals dicentric chromosomes generated by end-to-end chromosomal fusions that is a useful marker for loss of telomere integrity associated to age (Quintana-Sosa et al., 2021).

A progressive increase in MN frequency related to aging was observed in peritoneal T lymphocytes. This is in good agreement with previous studies in human populations reporting that MN production increases with age, as well as and in several neurological degenerative age-related diseases such as Alzheimer's and Parkinson's disease (Bonassi et al., 2011; Fenech and Bonassi, 2011). Although it has been reviewed that NPB frequency increases in normal aging due to a decrease in DNA repair capacity (Thomas et al., 2007), our findings show that telomere integrity is not mainly affected in the mice lymphocytes studied, because the NPB frequency observed was one order of magnitude lower than the frequency of MN formation. In addition, non-significant increase with aging was detected.

CBMN assay in combination with FISH using mouse pancentromeric probe shows a high frequency of Cen+MN, revealing that the major cause for MN formation in the lymphocytes analyzed is correct centromeric function failure, whereas MN without centromere sequences originated by fragments from chromosomal arms breakage are scarcely found. Taken all together, our data suggest that there is a chromosomal loss related to aging in mice that will lead to the formation of aneuploid lymphocytes. Different age-related causes can be addressed, such as mitotic spindle errors (Macedo et al., 2018) or dysfunctional cell cycle control proteins (Thompson et al., 2010). The positive correlation found between 1841MT signals and Cen+MN frequency suggests that the preferential insertion of the mitochondrial DNA sequences at the pericentromeric regions could affect segregation as well, contributing to the chromosome loss related to age. However, the mechanistic relationship between mtDNA insertions and chromosome instability remains to be elucidated. Moreover, the finding that the number of MN *per* cell does not increase with age is consistent with the results of Caro et al. (2010) who reported that age-related increase in mtDNA fragment insertion does not occur at random, but in definite regions where mtDNA is

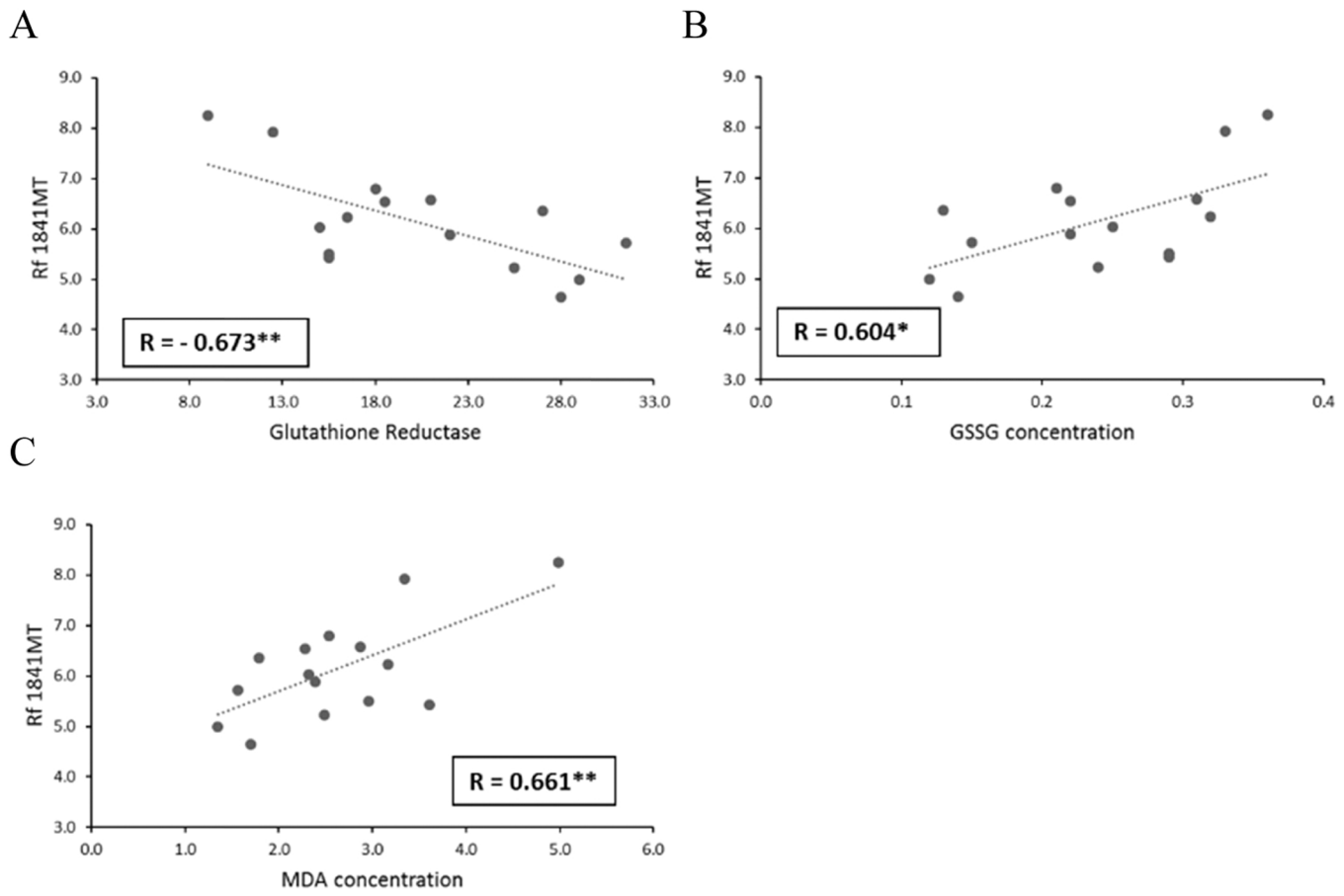

Fig. 5. Relationship between mtDNA relative fluorescence (Rf 1841MT) and A) Glutathione reductase activity (GR activity) B) Oxidized Glutathione (GSSG) concentration and C) Malondialdehyde (MDA) concentration. R=Pearsońs correlation coefficient; * : $p < 0.05$; **: $p < 0.01$.

already present. Later evidence has pointed out the role of DNA sequence microhomology in mitochondrial-nuclear DNA integration events (Ju et al., 2015).

An important fact to be analyzed is the consequence of an increasing genomic instability and MN formation in lymphocyte function and their implication in immunosenescence. We have observed an age-related decrease of the proliferative capacity of the lymphocytes, which is a typical marker of immunosenescence (Martinez de Toda et al., 2016), along with an increase in apoptosis, two related processes in these immune cells that become unbalanced with advancing aging (Ginaldi et al., 2000; Sikora, 2015). Our results agree with previous investigation reporting that genome instability and numerical chromosome changes, due to chromosome missegregation or loss, cause defective cell division, apoptosis and cell cycle arrest (Hanahan and Weinberg, 2011; George et al., 2014). Similarly, Bolognesi et al. (1999) confirmed the relation between the MN increase with age and the diminished proliferation in lymphocytes from both men and women. In this context, Decordier et al. (2002) demonstrated that MN trigger the elimination of micronucleated lymphocytes by directly inducing apoptosis. Our results seem to be consistent with this evidence, since a higher frequency of cells with cytological signs of late-stage apoptosis was observed at the old age.

The immunosenescence, and more concretely the lower proliferative capacity of response to T lymphocytes, is a consequence of the age-related oxidative stress (De la Fuente and Miquel, 2009). It is known that excessive and prolonged exposure to high ROS concentrations induces immune dysfunction, inhibiting T-cell proliferation and leading to apoptosis (Thorén et al., 2007). This chronic oxidative stress that occurs with age (with increasing ROS generation, together with a decline in antioxidant defenses) is associated with the oxidative damage to mtDNA, which has been considered the origin of the mitochondrial fragments (Singh et al., 2015) that can escape from the mitochondria towards the nucleus (Ritcher, 1988). Thus, in agreement with previous results (Martinez de Toda et al., 2020), lymphocytes of old animals showed more concentration of oxidants such as GSSG and MDA and less of the GR activity (a relevant antioxidant defense). Moreover, we find that these increased GSSG and MDA concentrations positively correlate with the mtDNA amounts detected in the nuclear genome of the lymphocytes analyzed, as well as, conversely, that the decreased GR activity negatively correlates with 1841MT amount.

Our results provide clues that allow us to propose a novel mechanism underlying immunosenescence in which mtDNA fragments, originated by the oxidative damage caused by the production of mitROS throughout the lifetime, accumulate inside the nuclear genome of T lymphocytes in a time-dependent way. The entrance of mitochondrial fragments at the pericentromeric regions may compromise chromosome segregation, causing genetic loss that leads to MN and aneuploid cell formation with reduced proliferation capacity.

The novelty of this proposal is worth mentioning because, to date, studies regarding insertions of mtDNA in the nuclear genome related to aging are scarce and circumscribed to the descriptive level. However, experimental mechanistic evidence of this phenomena is still needed, so further research deciphering this new mechanism will be the subject of our future investigations.

Additionally, and considering the need for clear, suitable and accurate indicators of biological age, our results point out the potential use of mtDNA fragment insertion in the nuclear genome as a cytogenetic parameter to be considered as a marker for biological age and longevity prediction.

Data Availability

Data will be made available on request.

Acknowledgments

We thank María J Puertas, Marcela Rosato and Thomas Gatewood for critically reading the manuscript. Thomas Gatewood for critically reading the manuscript. This work was supported by grants from the Ministerio de Economía y Competitividad, Spain, through the project MAT2016-76847-R, and from the Research Group of Universidad Complutense de Madrid (910379 "Envejecimiento, Neuroinmunología y Nutrición").

References

Bolognesi, C., Landini, E., Roggieri, P., Fabbri, R., Viarengo, A., 1999. Genotoxicity biomarkers in the assessment of heavy metal effects in mussels: experimental studies. Environ. Mol. Mutagen. 33 (4), 287–292. https://doi.org/10.1002/(SICI)1098-2280(1999)33:4.

Bonassi, S., Coskun, E., Ceppi, M., Lando, C., Bolognesi, C., Burgaz, S., Holland, N., Kirsch-Volders, M., Knasmueller, S., Zeiger, E., Carnesoltas, D., Cavallo, D., da Silva, J., de Andrade, V.M., Demircigil, G.C., Odio, A.D., Donmez-Altuntas, H., Gattas, G., Giri, A., Giri, S., Gómez-Meda, B., Gómez-Arroyo, S., Hadjidekova, V., Haveric, A., Kamboj, M., Kurteshi, K., Martino-Roth, M.G., Montoya, R.M., Nersesyan, A., Pastor-Benito, S., Salvadori, D.M.F., Shaposhnikova, A., Stopper, H., Thomas, P., Torres-Bugarín, O., Yadav, A.S., González, G.Z., Fenech, M., 2011. The HUman MicroNucleus project on eXfoLiated buccal cells (HUMN XL): The role of life-style, host factors, occupational exposures, health status, and assay protocol. Mutat. Res. 728 (3), 88–97. https://doi.org/10.1016/j.mrrev.2011.06.005.

Boveris, A., Oshino, N., Chance, B., 1972. The cellular production of hydrogen peroxide. Biochem. J. 128, 617–630. https://doi.org/10.1042/BJ1280617.

Brand, M.D., 2010. The sites and topology of mitochondrial superoxide production. Exp. Gerontol. 45 (7–8), 466–472. https://doi.org/10.1016/j.exger.2010.01.003.

Caro, P., Gómez, J., Arduini, A., González-Sánchez, M., González-García, M., Borrás, C., Viña, J., Puertas, M.J., Sastre, J., Barja, G., 2010. Mitochondrial DNA sequences are present inside nuclear DNA in rat tissues and increase with age. Mitochondrion 10, 479–486. https://doi.org/10.1016/j.mito.2010.05.004.

Catalán, J., Surrallés, J., C-MFalck, G., 2000. Segregation of sex chromosomes in human lymphocytes. Mutagenesis 15, 251–255. https://doi.org/10.1093/mutage/15.3.251.

Catalán, J., Autio, K., Wessman, M., Lindholm, C., Knuutila, S., Sorsa, M., Norppa, H., 1995. Age-associated micronuclei containing centromeres and the X chromosome in lymphocytes of women. Cytogenet. Cell Genet. 68 (1–2), 11–16. https://doi.org/10.1159/000133879.

Cheng, X., Ivessa, A.S., 2010. The migration of mitochondrial DNA fragments to the nucleus affects the chronological aging process of Saccharomyces cerevisiae. Aging Cell 9, 919–923. https://doi.org/10.1111/j.1474-9726.2010.00607.x.

Cheng, X., Ivessa, A.S., 2012. Accumulation of linear mitochondrial DNA fragments in the nucleus shortens the chronological life span of yeast. Eur. J. Cell Biol. 91, 782–788. https://doi.org/10.1016/j.ejcb.2012.06.005.

Cottliar, A.S., Slavutsky, I.R., 2001. Telomeres and telomerase activity: their role in aging and in neoplastic development. Medicina 61 (3), 335–342.

De La Fuente, M., Miquel, J., 2009. An update of the oxidation-inflammation theory of aging: the involvement of the immune system in oxi-inflamm-aging. Curr. Pharm. Des. 15, 3003–3026. https://doi.org/10.2174/138161209789058110.

Decordier, I., Dillen, L., Cundari, E., Kirsch-Volders, M., 2002. Elimination of micronucleated cells by apoptosis after treatment with inhibitors of microtubules. Mutagenesis 17 (4), 337–344. https://doi.org/10.1093/mutage/17.4.337.

Fenech, M., 2007. Cytokinesis-block micronucleus cytome assay. Nat. Protoc. 2, 1084–1104. https://doi.org/10.1038/nprot.2007.77.

Fenech, M., Bonassi, S., 2011. The effect of age, gender, diet and lifestyle on DNA damage measured using micronucleus frequency in human peripheral blood lymphocytes. Mutagenesis 26 (1), 43–49. https://doi.org/10.1093/mutage/geq050.

Fenech, M., Chang, W.P., Kirsch-Volders, M., Holland, N., Bonassi, S., Zeiger, E., 2003. HUMN project: detailed description of the scoring criteria for the cytokinesis-block micronucleus assay using isolated human lymphocyte cultures. Mutat. Res. /Genet. Toxicol. Environ. Mutagen. 534, 65–75. https://doi.org/10.1016/S1383-5718(02)00249-8.

Fenech, M., Holland, N., Kirsch-Volders, M., Knudsen, L.E., Wagner, K.H., Stopper, H., Knasmueller, S., Bolognesi, C., El-Zein, R., Bonassi, S., 2020. Micronuclei and disease – Report of HUMN project workshop at Rennes 2019 EEMGS conference. Mutat. Res. - Genet. Toxicol. Environ. Mutagen. 850–851. https://doi.org/10.1016/j.mrgentox.2020.503133.

Fukagawa, T., Earnshaw, W.C., 2014. The centromere: Chromatin foundation for the kinetochore machinery. Dev. Cell 30 (5), 496–504. https://doi.org/10.1016/j.devcel.2014.08.016.

Garagna, S., Zuccotti, M., Capanna, E., Redi, C.A., 2002. High-resolution organization of mouse telomeric and pericentromeric DNA. Cytogenet. Genome Res. 112 (3–4), 248–255. https://doi.org/10.1159/000089878.

Garrido, A., Cruces, J., Ceprián, N., Hernández-Sánchez, C., De la Fuente, M., 2018. Premature aging in behaviour and immune functions in tyrosine hydroxylase haploinsufficient female mice. A longitudinal study. Brain, Behav., Immun. 69, 440–455. https://doi.org/10.1016/j.bbi.2018.01.003.

George, A., Dey, R., Bhuria, V., Banerjee, S., Ethirajan, S., Siluvaimuthu, A., Saraswathy, R., 2014. Nuclear anomalies, chromosomal aberrations and proliferation rates in cultured lymphocytes of head and neck cancer patients. Asian Pac. J. Cancer Prev.: APJCP 15 (3), 1119–1123. https://doi.org/10.7314/apjcp.2014.15.3.1119.

Ginaldi, L., de Martinis, M., D'Ostilio, A., Marini, L., Loreto, M.F., Corsi, M.P., Quaglino, D., 2000. Cell proliferation and apoptosis in the immune system in the elderly. Immunol. Res. 21, 31–38. https://doi.org/10.1385/IR:21:1:31.

Guenatri, M., Bailly, D., Maison, C., Almouzni, G., 2004. Mouse centric and pericentric satellite repeats form distinct functional heterochromatin. J. Cell Biol. 166, 493–505. https://doi.org/10.1083/jcb.200403109.

Hanahan, D., Weinberg, R.A., 2011. Hallmarks of cancer: the next generation. Cell 144, 646–674. https://doi.org/10.1016/J.CELL.2011.02.013.

Harman, D., 1972. The Biologic Clock: The Mitochondria? J. Am. Geriatr. Soc. 20, 145–147. https://doi.org/10.1111/J.1532-5415.1972.TB00787.X.

Harrison, D.E., Strong, R., Sharp, Z.D., Nelson, J.F., Astle, C.M., Flurkey, K., Nadon, N.L., Wilkinson, J.E., Frenkel, K., Carter, C.S., Pahor, M., Javors, M.A., Fernandez, E., Miller, R.A., 2009. Rapamycin fed late in life extends lifespan in genetically heterogeneous mice. Nature 460, 392–395. https://doi.org/10.1038/nature08221.

Harutyunyan, T., Al-Rikabi, A., Sargsyan, A., Hovhannisyan, G., Aroutiounian, R., Liehr, T., 2020. Doxorubicin-induced translocation of mtDNA into the nuclear genome of human lymphocytes detected using a molecular-cytogenetic approach. Int. J. Mol. Sci. 21, 1–11. https://doi.org/10.3390/ijms21207690.

Hastings, P.J., Ira, G., Lupski, J.R., 2009. A microhomology-mediated break-induced replication model for the origin of human copy number variation. PLoS Genet. 5 (1), e1000327 https://doi.org/10.1371/journal.pgen.1000327.

Hazkani-Covo, E., Zeller, R.M., Martin, W., 2010. Molecular poltergeists: mitochondrial DNA copies (NUMTs) in sequenced nuclear genomes. PLoS Genet. 6, e1000834 https://doi.org/10.1371/JOURNAL.PGEN.1000834.

Hunter, D.R., Haworth, R.A., 1979. The Ca2+-induced membrane transition in mitochondria: I. The protective mechanisms. Arch. Biochem. Biophys. 195, 453–459. https://doi.org/10.1016/0003-9861(79)90371-0.

Ijdo, J.W., Baldini, A., Ward, D.C., Reeders, S.T., Wells, R.A., 1991. Origin of human chromosome 2: an ancestral telomere-telomere fusion. Proc. Natl. Acad. Sci. USA 88, 9051–9055. https://doi.org/10.1073/PNAS.88.20.9051.

Ju, Y.S., Tubio, J.M.C., Mifsud, W., Fu, B., Davies, H.R., Ramakrishna, M., Li, Y., Yates, L., Gundem, G., Tarpey, P.S., Behjati, S., Papaemmanuil, E., Martin, S., Fullam, A., Gerstung, M., Nangalia, J., Green, A.R., Caldas, C., Borg, Å., Tutt, A., Michael Lee, M.T., Van'T Veer, L.J., Tan, B.K.T., Aparicio, S., Span, P.N., Martens, J. W.M., Knappskog, S., Vincent-Salomon, A., Børresen-Dale, A.L., Eyfjörd, J.E., Flanagan, A.M., Foster, C., Neal, D.E., Cooper, C., Eeles, R., Lakhani, S.R., Desmedt, C., Thomas, G., Richardson, A.L., Purdie, C.A., Thompson, A.M., McDermott, U., Yang, F., Nik-Zainal, S., Campbell, P.J., Stratton, M.R., 2015. Frequent somatic transfer of mitochondrial DNA into the nuclear genome of human cancer cells. In: Genome Research, 25, pp. 814–824. https://doi.org/10.1101/gr.190470.115.

Kuznetsova, I., Podgornaya, O., Ferguson-Smith, M.A., 2006. High-resolution organization of mouse centromeric and pericentromeric DNA. Cytogenet. Genome Res. 112, 248–255. https://doi.org/10.1159/000089878.

Latorre, A., Moya, A., Ayala, F.J., 1986. Evolution of mitochondrial DNA in Drosophila subobscura. Proc. Natl. Acad. Sci. 83, 8649–8653. https://doi.org/10.1073/pnas.83.22.8649.

Liu, L., Keefe, D.L., 2008. Defective cohesin is associated with age-dependent misaligned chromosomes in oocytes. Reprod. Biomed. Online 16, 103–112. https://doi.org/10.1016/S1472-6483(10)60562-7.

Macedo, J.C., Vaz, S., Bakker, B., Ribeiro, R., Bakker, P.L., Escandell, J.M., Ferreira, M. G., Medema, R., Foijer, F., Logarinho, E., 2018. FoxM1 repression during human aging leads to mitotic decline and aneuploidy-driven full senescence. Nat. Commun. 9, 2834. https://doi.org/10.1038/s41467-018-05258-6.

Martínez de Toda, I., Vida, C., Miguel, L.S.S., de La Fuente, M., 2019. Function, oxidative, and inflammatory stress parameters in immune cells as predictive markers of lifespan throughout aging. Oxid. Med. Cell. Longev. 2019. https://doi.org/10.1155/2019/4574276.

Martínez de Toda, I., Vida, C., Garrido, A., de La Fuente, M., 2020. Redox parameters as markers of the rate of aging and predictors of life Span. J. Gerontol. - Ser. A Biol. Sci. Med. Sci. 75, 613–620. https://doi.org/10.1093/gerona/glz033.

Martínez de Toda, I., Ceprián, N., Díaz-Del Cerro, E., de la Fuente, M., 2021. The role of immune cells in oxi-inflamm-aging. Cells 10, 2974. https://doi.org/10.3390/cells10112974.

Martínez de Toda, I., Maté, I., Vida, C., Cruces, J., de la Fuente, M., 2016. Immune function parameters as markers of biological age and predictors of longevity. Aging 8, 3110–3119. https://doi.org/10.18632/aging.101116.

Martínez-Cisuelo, V., Gómez, J., García-Junceda, I., Naudí, A., Cabré, R., Mota-Martorell, N., López-Torres, M., González-Sánchez, M., Pamplona, R., Barja, G., 2016. Rapamycin reverses age-related increases in mitochondrial ROS production at complex I, oxidative stress, accumulation of mtDNA fragments inside nuclear DNA, and lipofuscin level, and increases autophagy, in the liver of middle-aged mice. Exp. Gerontol. 83, 130–138. https://doi.org/10.1016/j.exger.2016.08.002.

Matsuo, M., Ito, Y., Yamauchi, R., Obokata, J., 2005. The rice nuclear genome continuously integrates, shuffles, and eliminates the chloroplast genome to cause chloroplast-nuclear DNA flux. Plant Cell 17, 665–675. https://doi.org/10.1105/tpc.104.027706.

Michalovova, M., Vyskot, B., Kejnovsky, E., 2013. Analysis of plastid and mitochondrial DNA insertions in the nucleus (NUPTs and NUMTs) of six plant species: Size, relative

age and chromosomal localization. Heredity 111, 314–320. https://doi.org/10.1038/hdy.2013.51.
Migliore, L., Cocchi, L., Scarpato, R., 1996. Detection of the centromere in micronuclei by fluorescence in situ hybridization: its application to the human lymphocyte micronucleus assay after treatment with four suspected aneugens. Mutagenesis 11 (3), 285–290. https://doi.org/10.1093/mutage/11.3.285.
Moro-García, M.A., Mayo, J.C., Sainz, R.M., Alonso-Arias, R., 2018. Influence of inflammation in the process of T lymphocyte differentiation: proliferative, metabolic, and oxidative changes. Front. Immunol. 9, 339. https://doi.org/10.3389/FIMMU.2018.00339/BIBTEX.
Patrushev, M., Kasymov, V., Patrusheva, V., Ushakova, T., Gogvadze, V., Gaziev, A., 2004. Mitochondrial permeability transition triggers the release of mtDNA fragments. Cell. Mol. Life Sci. 61, 3100–3103. https://doi.org/10.1007/s00018-004-4424-1.
Pawelec, G., 2018. Age and immunity: What is "immunosenescence"? Exp. Gerontol. 105, 4–9. https://doi.org/10.1016/J.EXGER.2017.10.024.
Pellestor, F., Andréo, B., Arnal, F., Humeau, C., Demaille, J., 2003. Maternal aging and chromosomal abnormalities: new data drawn from in vitro unfertilized human oocytes. Hum. Genet. 112, 195–203. https://doi.org/10.1007/s00439-002-0852-x.
Peters, H.F.M., O'Carroll, D., Scherthan, H., Mechtler, K., Sauer, S., Schöfer, C., Weipoltshammer, K., Pagani, M., Lachner, M., Kohlmaier, A., Opravil, S., Doyle, M., Sibilia, M., Jenuwein, T., 2001. Loss of the Suv39h histone methyltransferases impairs mammalian heterochromatin and genome stability. Cell 107 (3), 323–337. https://doi.org/10.1016/S0092-8674(01)00542-6.
Puertas, M.J., González-Sánchez, M., 2020. Insertions of mitochondrial DNA into the nucleus—effects and role in cell evolution. Genome 63, 365–374. https://doi.org/10.1139/gen-2019-0151.
Quintana-Sosa, M., León-Mejía, G., Luna-Carrascal, J., de Moya, Y.S., Rodríguez, I.L., Acosta-Hoyos, A., Anaya-Romero, M., Trindade, C., Narváez, D.M., Restrepo, H.G. de, Dias, J., Niekraszewicz, L., Garcia, A.L.H., Rohr, P., da Silva, J., Henriques, J.A. P., 2021. Cytokinesis-block micronucleus cytome (CBMN-CYT) assay biomarkers and telomere length analysis in relation to inorganic elements in individuals exposed to welding fumes. Ecotoxicol. Environ. Saf. 212, 111935 https://doi.org/10.1016/J.ECOENV.2021.111935.
Ricchetti, M., Fairhead, C., Dujon, B., 1999. Mitochondrial DNA repairs double strand breaks in yeast chromosomes. Nature 402, 96–100. https://doi.org/10.1038/47076.
Richter, C., 1988. Do mitochondrial DNA fragments promote cancer and aging? Fed. Eur. Biochem. Soc. 241, 1–5.
Rickwood, D.W., Wilson, M.T., Darley-Usmar, V.M., 1987. Isolation and characteristics of intact mitochondria. In: Darley-usmar, V.M., Wilson, M.T., Rickwood, D. (Eds.), Mitochondria: A Practical Approach. IRL Press, Oxford, pp. 4–6.
Sanchez-Roman, I., Barja, G., 2013. Regulation of longevity and oxidative stress by nutritional interventions: role of methionine restriction. Exp. Gerontol. 48, 1030–1042. https://doi.org/10.1016/j.exger.2013.02.021.
Shay, J.W., Werbin, H., 1992. New evidence for the insertion of mitochondrial DNA into the human genome: significance for cancer and aging. Mutat. Res. /DNAging 275, 227–235. https://doi.org/10.1016/0921-8734(92)90026-L.
Sikora, E., 2015. Activation-induced and damage-induced cell death in aging human T cells. Mech. Ageing Dev. 151, 85–92. https://doi.org/10.1016/J.MAD.2015.03.011.
Singh, G., Pachouri, U.C., Khaidem, D.C., Kundu, A., Chopra, C., Singh, P., 2015. Mitochondrial DNA damage and diseases. F1000Research 4, 176. https://doi.org/10.12688/f1000research.6665.
Singh, K.K., Choudhury, A.R., Tiwari, H.K., 2017. Numtogenesis as a mechanism for development of cancer. Semin. Cancer Biol. 47, 101–109. https://doi.org/10.1016/j.semcancer.2017.05.003.
Suter, M., Richter, C., 1999. Fragmented mitochondrial DNA is the predominant carder of oxidized DNA bases. Biochemistry 38, 459–464. https://doi.org/10.1021/bi9811922.
Taddei, A., Maison, C., Roche, D., Almouzni, G., 2001. Reversible disruption of pericentric heterochromatin and centromere function by inhibiting deacetylases. Nat. Cell Biol. 3 (2), 114–120. https://doi.org/10.1038/35055010.
Thomas, P., Harvey, S., Gruner, T., Fenech, M., 2007. The buccal cytome and micronucleus frequency is substantially altered in Down's syndrome and normal ageing compared to young healthy controls. Mutat. Res. - Fundam. Mol. Mech. Mutagen. 638, 37–47. https://doi.org/10.1016/j.mrfmmm.2007.08.012.
Thompson, S.L., Bakhoum, S.F., Compton, D.A., 2010. Mechanisms of chromosomal instability. Curr. Biol. 20 (6), 285–295. https://doi.org/10.1016/j.cub.2010.01.034.
Thorén, F.B., Betten, Å., Romero, A.I., Hellstrand, K., 2007. Cutting edge: antioxidative properties of myeloid dendritic cells: protection of T cells and NK cells from oxygen radical-induced inactivation and apoptosis. J. Immunol. 179, 21–25. https://doi.org/10.4049/JIMMUNOL.179.1.21.
Turner, C., Killoran, C., Thomas, N.S.T., Rosenberg, M., Chuzhanova, N.A., Johnston, J., Kemel, Y., Cooper, D.N., Biesecker, L.G., 2003. Human genetic disease caused by de novo mitochondrial-nuclear DNA transfer. Hum. Genet. 112, 303–309. https://doi.org/10.1007/s00439-002-0892-2.
Vermot, A., Petit-Härtlein, I., Smith, S.M.E., Fieschi, F., 2021. NADPH Oxidases (NOX): an overview from discovery, molecular mechanisms to physiology and pathology. Antioxidants 10 (6), 890. https://doi.org/10.3390/antiox10060890.
Vig, B.K., 1982. Sequence of centromere separation: role of centromeric heterochromatin. Genetics 102 (4), 795–806. https://doi.org/10.1093/genetics/102.4.795.